doi:10.1016/j.jmb.2003.07.012 J. Mol. Biol. (2003) 332, 1175–1182

JMB

Available online at www.sciencedirect.com

SCIENCE DIRECT®

ELSEVIER

# The Crystallographic Structure of Na,K-ATPase N-domain at 2.6 Å Resolution

**Kjell O. Håkansson**

*August Krogh Institute*
*Copenhagen University*
*Universitetsparken 13*
*DK-2100 Copenhagen OE*
*Denmark*

The structure of the N-domain of porcine $\alpha_2$ Na,K-ATPase was determined crystallographically to 3.2 Å resolution by isomorphous heavy-atom replacement using a single mercury derivative. The structure was finally refined against 2.6 Å resolution synchrotron data. The domain forms a seven-stranded antiparallel β-sheet with two additional β-strands forming a hairpin and five α-helices. Approximately 75% of the residues were superimposable with residues from the structure of Ca-ATPase N-domain, and a structure-based sequence alignment is presented. The positions of key residues are discussed in relation to the pattern of hydrophobicity, charge and sequence conservation of the molecular surface. The structure of a hexahistidine tag binding to nickel ions is presented.



*Keywords:* Na,K-ATPase structure; crystallography; HisTag; ATP binding; membrane protein

## Introduction

Na,K-ATPase is an integral membrane protein that uses energy from ATP-hydrolysis to transport $Na^+$ out of and $K^+$ into the cell.[1–3] Na,K-ATPase belongs to the P-type ATPases and consists of ten transmembrane helices and three cytoplasmic domains. The A-domain is formed by the segment between transmembrane helices 2 and 3 together with the N terminus. A larger cytoplasmic loop between transmembrane helices 4 and 5 forms the P-domain into which the N-domain is inserted. The N-domain binds the ATP nucleotide substrate, and the P-domain contains an aspartic acid residue that is phosphorylated transiently, followed by release of ADP from the N-domain and hydrolysis of the phosphoaspartic acid residue on the P-domain. This chain of events is coupled to the active export of three sodium ions and import of two potassium ions between the transmembrane helices across the cell membrane. The domains undergo large rigid-body movements during this transport cycle, alternating between two conformations, which are referred to as E1 and E2, respectively.[4,5] The only P-type ATPase for which a crystallographic structure has been published is rabbit sarcoplasmic reticulum Ca-ATPase, which has been crystallised in both the E1 and E2 conformations.[6,7] Similar structural organisation and conformational changes have been visualised by a number of electron microscopy studies of Na,K-ATPase, Ca-ATPase and related ATPases.[8–11] The present study describes the crystallographic structure of the N-domain of porcine $\alpha_2$ Na,K-ATPase, representing the first crystallographic structural data available on the Na,K-ATPase ion pump.

Abbreviation used: SIR, single isomorphous replacement.

E-mail address of the corresponding author: kohakansson@aki.ku.dk

## Results

### Structure of the hexa-histidine tag and crystal packing

Both the N-terminal methionine residue and the C-terminal $His_6$ tag are involved in intermolecular interactions in the crystal. The structure of the $His_6$ tag with bound $Ni^{2+}$ is crucial for these interactions and explains why $Ni^{2+}$ is essential for crystallisation. There are two nickel ions on special positions on the cubic 3-fold symmetry axis, which tie together three asymmetric units, as shown in Figure 1(a) and (b). Both of these nickel ions are octahedrally coordinated by six histidine residues, two from each molecule. The first $Ni^{2+}$ is coordinated by His587 and His589 from all three molecules, and the second $Ni^{2+}$ is coordinated by His590 and His592. The coordinating distances are 2.1 Å for the first of these

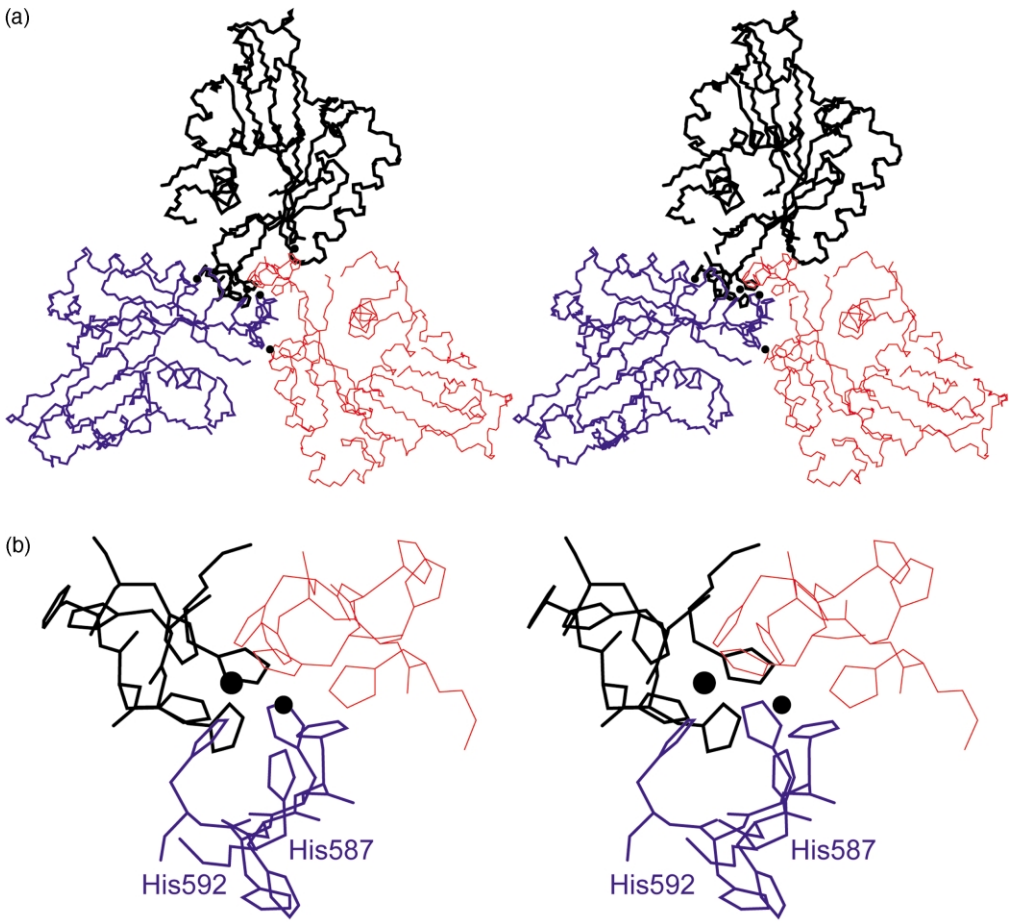


**Figure 1**. (a) Structure of the nickel-complexed $His_6$ tag. Three molecules, one from each of three asymmetric units, are drawn in different colour and line thickness. Only the backbone, nickel ions (black spheres) and the nickel-coordinating side-chains are shown. Two nickel ions on special positions on the crystallographic 3-fold axis can be seen in the centre of the image, coordinated to all three molecules. The third nickel ion bridging two adjacent molecules can, as a result of the 3-fold symmetry, be seen at all three molecule interfaces. (b) Close-up of the nickel site, demonstrating the octahedral coordination of the two nickel ions on special positions. The 3-fold axis runs through the two nickel ions shown.

nickel ions and between 2.0 Å and 2.4 Å for the second, with angles ranging from 85° to 95°. The remaining two histidine residues, 588 and 591, coordinate a third nickel ion, which is not on a special position, but is situated on the interface between two N-domains, where it interacts with the internal residues His383 and Glu392 from the neighbouring molecule. These ligands are roughly in a plane, and are joined with an apical water molecule. It is possible that higher-resolution data would reveal another apical water molecule, in which case the coordination would be octahedral also for this $Ni^{2+}$. Metal–ligand distances are 2.0–2.2 Å and His $N^{\varepsilon 2}$–$Ni^{2+}$–His $N^{\varepsilon 2}$ and His $N^{\varepsilon 2}$–$Ni^{2+}$–water angles range from 81° to 97°. The Glu392 ligand residue has a bidentate character, in that the second carboxylate oxygen atom approaches the $Ni^{2+}$ at 3.0 Å and deviates more from octahedral geometry than the other ligands. Thus, no more than two histidine residues from the same molecules interact with the same $Ni^{2+}$, and internal histidine residues and carboxylate groups can contribute to protein–nickel interactions. In terms of secondary structure, the $His_6$ tag can be described as two short, three residue pieces in β-strand conformation, although the backbone does not hydrogen bond. The first and third of the histidine residues in each of these two segments form a complex with the same nickel ion, while the second histidine residue (i.e. second and fifth in the $His_6$ tag) coordinates to the nickel ion that is not in a special position.

## Structure of the Na,K-ATPase N-domain

The fold of the domain can be described as a seven-stranded antiparallel β-sheet, with an additional hairpin consisting of two β-strands. These two β-strands are continuous with the β-sheet, where they replace strands 1 and 2 at one corner of the sheet, resulting in a bifurcated β-sheet. The ribbons representation in Figure 2(a) demonstrates the topology of the domain, while

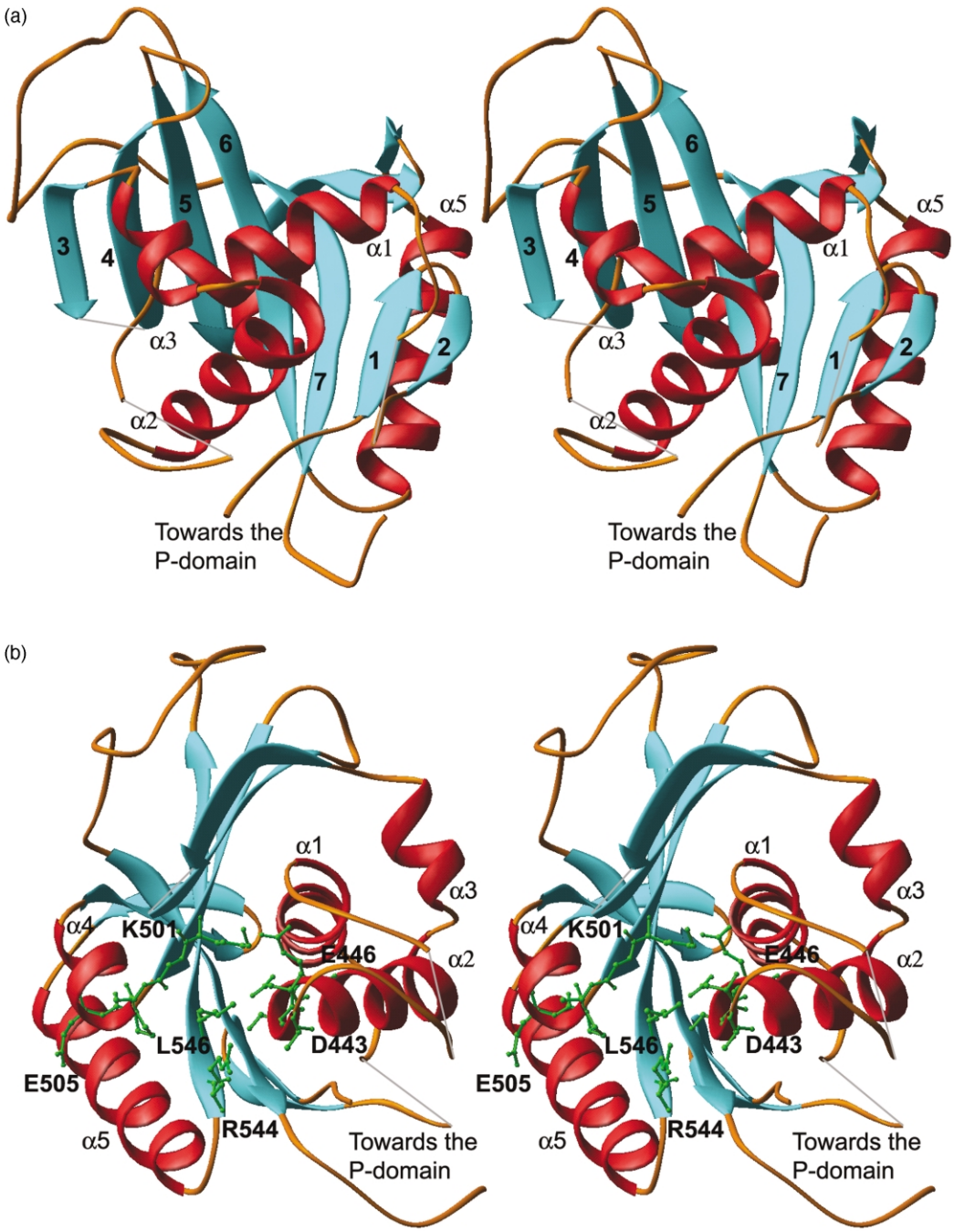


**Figure 2**. Ribbons representations[29] of Na,K-ATPase N-domain. (a) View normal to the β-sheet. The β-strands are numbered 1–7 and the α-helices are numbered 1–5 (α4 is on the back side). For clarity, gaps in the structure have been "mended" with grey straight lines. (b) View more or less along the β-sheet, from the left in the previous Figure. Strand β3 is closest to the viewer, followed by β4, β5, β6, β7, β1 and β2. The conserved motifs 443DASE, 501KGAPE and 544RXL are shown as green stick-and-ball.

Figure 2(b) shows the positions of some key residues. Figure 3 shows a backbone structure-based sequence alignment of Na,K-ATPase N-domain and the homologous Ca-ATPase (pdb entry 1EUL).[6] Due to the low level of sequence similarity, the alignment is very different from those obtained through standard sequence alignment protocols, particularly in the first half of the sequences. Superimposition of the $C^{\alpha}$ atoms of the structurally aligned residues results in an r.m.s. deviation of $C^{\alpha}$ atoms of 1.3 Å. There is only a limited number of conserved residues, i.e. identical or similar amino acids in structurally homologous position, and inspection of the positions of these residues will indicate whether they can interact with the substrate.

The Na,K-ATPase domain starts at residue 378, where the naturally occurring arginine has been replaced by methionine in order to allow translation of the gene. The first β-strand contains three

residues that are conserved in porcine Na,K-ATPase and rabbit sarcoplasmic reticulum Ca-ATPase. These residues, Met379, Val381 and Met384, are all hydrophobic and, due to a β-bulge, where Ala382 is in α-helical conformation, Val381 and the totally buried Met384 are both directed away from the surface. Strand β2, which is adjacent to the first strand, contains no conserved residues and is therefore unlikely to play a major role in ATP binding. In Ca-ATPase, there is one more relatively small β-strand at the edge of the β-sheet, but this part of the structure has lost its β-conformation in Na,K-ATPase. It is unlikely that the short, disordered Glu397-Ala402 loop will form a β-strand, since there would be no neighbouring segment in β-conformation within hydrogen bond distance. This random-coil structure is followed by an amphipathic α-helix with five conserved residues. Three of these, the hydrophobic Leu414, Ile417 and Leu420, are involved in packing the helix against the β-strands β4, β5, β6 and β7. Asn422 at the C-terminal end of the helix hydrogen bonds to the likewise conserved Arg464 side-chain. In Ca-ATPase, this helix is followed by a β-hairpin, but in the Na,K-ATPase structure this segment is disordered. The beginning of the second α-helix consists of residues that are either strictly conserved or very similar in the two enzymes. The hydrophilic Asp(Glu)443, Ser(Thr)445 and Glu446 in this conserved sequence motif are directed towards the hydrophobic pocket, away from the N–P-domain junction. Following the subsequent α3 helix are the β3-β4-β5-strands, forming a β-meander motif moving from the edge of the β-sheet towards the centre. The Phe475-Lys480 stretch, which includes the end of β3 and beginning of β4, is disordered but, since the residues on each side of this gap superimpose well with the corresponding residues in Ca-ATPase, the turn can be modelled with some confidence. Strand β4 is devoid of conserved residues. Strand β5, on the other hand, ends with a conserved KGAPE motif. Lys501 hydrogen bonds to the side-chain of Glu446 of the α2 helix and the backbone carbonyl group of Cys421 of the α1 helix. The conformation of Gly502 in the Na,K-ATPase, but not in Ca-ATPase,[6] is in a region of the Ramachandran plot where the presence of a side-chain would be unfavourable. It is not clear why Pro504 and Glu505 are conserved, but the presence of a proline residue between β5 and the subsequent α4-helix might be structurally important. The inability of Pro504 to function as a hydrogen bond donor breaks up the β5-β6 interaction, thereby creating the ATP-binding site pocket, at the same time preventing a premature start of helix α4. The region between β5 and β6 contains a β-hairpin (*vide supra*) hydrogen bonded to strand β7. The beginning of strand β6 contains two conserved key residues, Arg544 and Leu546, both involved in defining the surface of the ATP-binding pocket. The last strand β7 joins strands β6 and β1 in the centre of the β-sheet and returns towards the P-domain. Conserved residues in this strand are more or less buried hydrophobic residues, with the exception of Asp586 at the N–P domain junction.

Several attempts to bind nucleotides to the N-domain were made, including co-crystallisation with ATP, soaking crystals in ATP and $Mg^{2+}$, soaking with ADP and soaking with ADPNP. No density attributable to ligand was found in any of these structures.

## Discussion

The structure of the Na,K-ATPase N-domain enables us to examine the positions of some essential residues, which have been discovered through chemical modification or site-directed mutagenesis. Covalent labelling of Lys480 with the affinity labelling reagents pyridoxal-5′-diphospho-5-adenosine, pyridoxal-5′-phosphate and the photoaffinity reagent 8-azido-ATP result in loss of enzymatic activity.[12,13] The enzyme is protected from these reagents by the presence of ATP, but mutation of Lys480 has only a small effect on ATP binding.[14] These results suggest that the residue is close to, but perhaps not directly interacting with, bound ATP. In the three-dimensional structure, this is part of the Phe475-Lys480 hairpin, confining the hydrophobic pocket opposite the P-domain. Another residue that can be modified with loss of activity is Lys501.[15] Although mutation of Lys501 to Glu reduces the affinity for ATP,[16] replacement of the homologous Lys515 in Ca-ATPase with Ala has no effect on ATP binding.[17] The solvent-accessibility of this residue, which hydrogen bonds to Glu446, is low and the effect of chemical modification might again be the result of the introduction of a bulky group in the active site and not necessarily meaning that Lys501 interacts directly with ATP. Another key residue is the charged Arg544; mutation of this residue to Gln has a drastic effect on both ATP and ADP-binding, whereas R544K mutations have reduced ADP but intact ATP affinity.[18] The positions of hydrophobic residues in and around the active site are indicated in the surface representation in Figure 4(a), and the positions of hydrophilic residues are indicated in Figure 4(b), along with the electrostatic potential of the molecular surface. Figure 4(c) finally shows the surface distribution of residues that are conserved in porcine $\alpha_2$ Na,K-ATPase and rabbit sarcoplasmic reticulum Ca-ATPase, according to the alignment in Figure 3.

The transition from the E1 to the E2 conformation involves the collective movement of the N and P-domains towards the A-domain. The crystallographic structures of Ca-ATPase in the E1 and in the E2 conformation show that the gap between the N and P-domain in the E1 form is narrowed in the E2 form.[6,7] Involvement of the N-domain in crystal packing can have promoted the large separation of the two domains in the E1 form and, since domain closure appears necessary for ATP bound

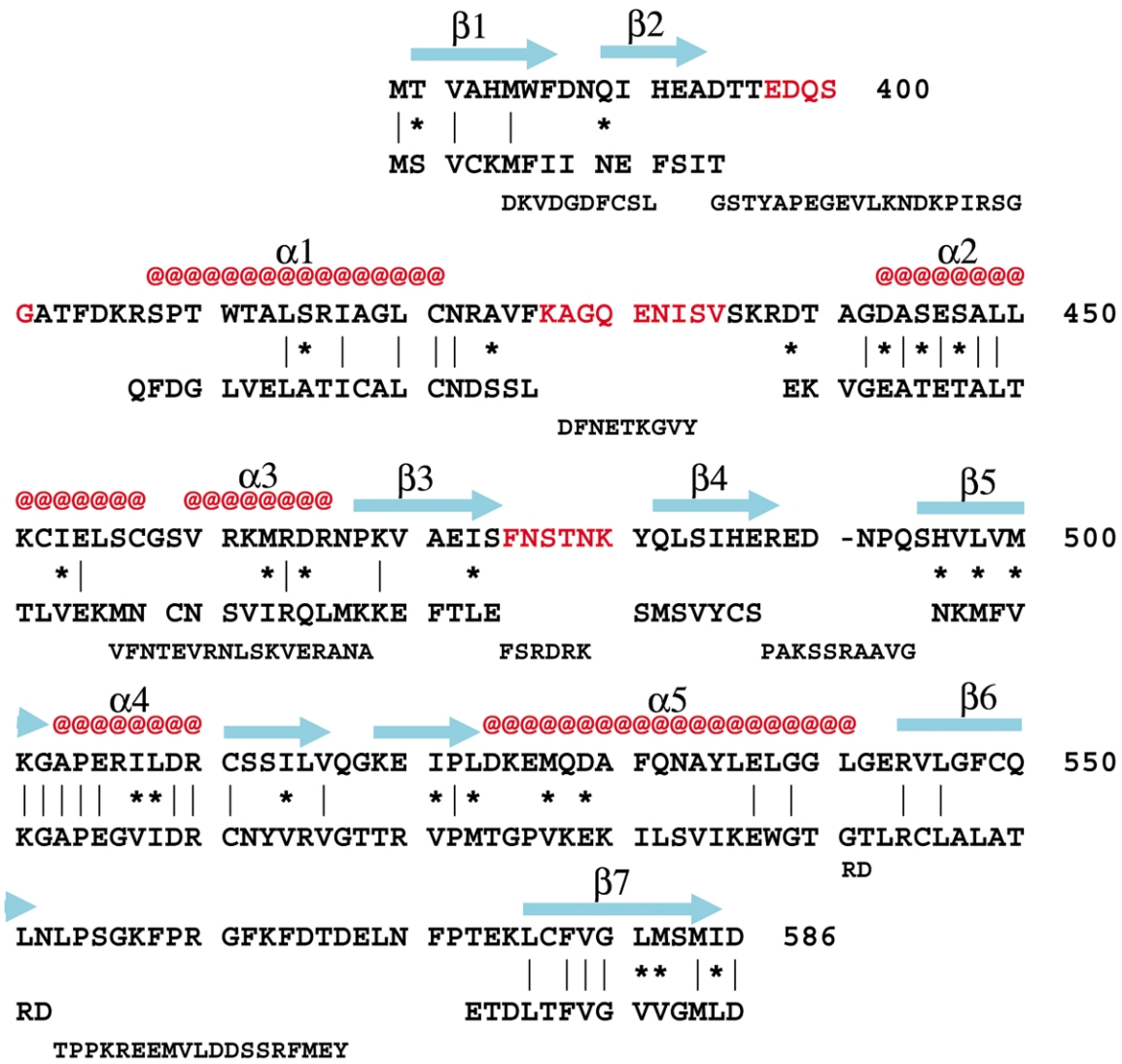


**Figure 3**. Structure-based alignment of porcine $\alpha_2$ Na,K-ATPase N-domain and rabbit sarcoplasmic reticulum Ca-ATPase N-domain.[6] The numbering used here is the same as for the $\alpha_1$ isoform. Residues are aligned according to the local backbone structure, and homologous residues in the β-sheet make similar hydrogen contacts with other strands in the two proteins. Helices are represented with @ in red, and β-strands as blue arrows. The two β-strands that are not numbered belong to the hairpin loop described in the text and shown in the upper right of Figure 2(a). Ca-ATPase residues that could not be aligned with Na,K-ATPase are shown is smaller letters below the lines of aligned residues. Matches between the two proteins are marked with a |, and residues that belong to the same of the five groups (S,A,T), (D,E,N,Q,H), (K,R), (V,M,I,L) and (F,Y) with ∗. Residues that lacked interpretable electron density are shown in red.

on the N-domain to reach the phosphorylation residue Asp369 on the P-domain, it is reasonable to assume that this takes place before phosphorylation and prior to E1-E2 transition. Thus, an approximate position for the P-domain and the phosphorylation residue relative to the N-domain can be found through superimposition of the N-domain of Na,K-ATPase and the N-P-domains of the crystallographic structure of E2 Ca-ATPase, pdb entry 1IWO. The P-domain in the closed form would, from below, shadow much of the N-domain surface, as displayed in Figure 4(a)–(c). The trimodal pattern of hydrophobicity around Leu546-Ala503, positive charge at Arg544 and negative charge at the α2 helix is conserved in both Na,K-ATPase and Ca-ATPase, as the RXL, KGAPE and GD/(E)AS/(T)E motifs. The hydrophobic, conserved and essential Phe475[19] is also a part of this hydrophobic patch. The negative charge of Asp443 and Glu446, situated at the N terminus of helix α2, is counteracted by the helical dipole moment. The surface properties and the conservation pattern suggest a hydrophobic-binding site at the area around Leu546 suitable for an adenine ring, a hydrophilic site at the N terminus of helix α2 suitable for a ribose ring, and a positively charged site at Arg544 for the phosphate chain. Actually, placing an ATP molecule in

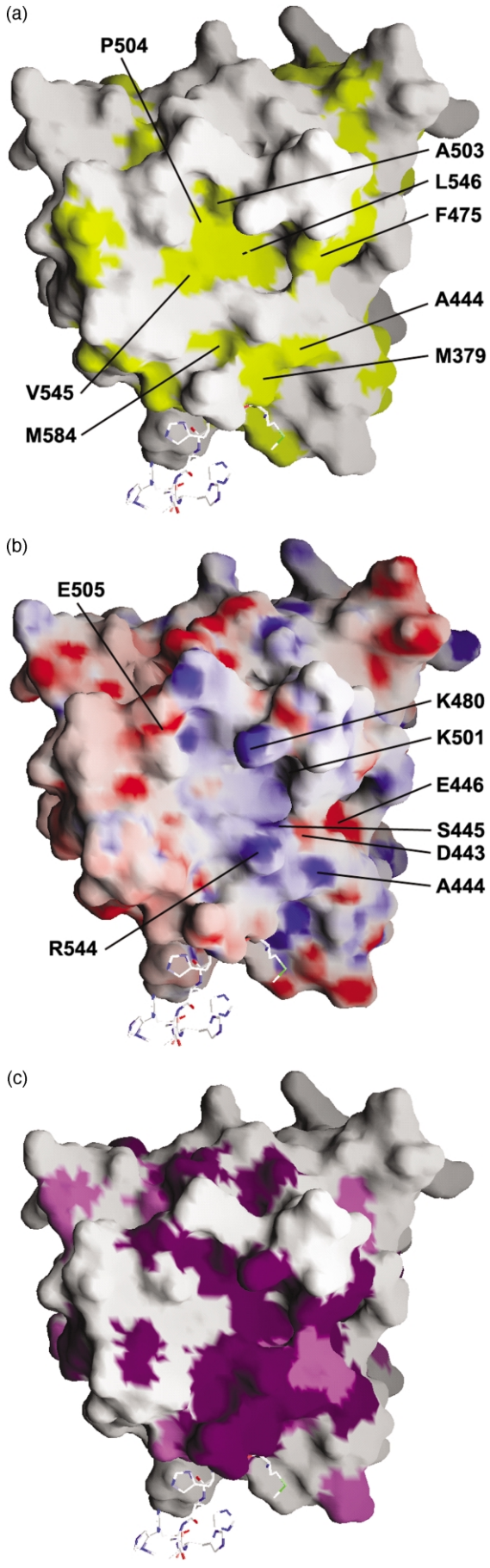


this manner with an extended phosphate chain will position the γ-phosphate group next to the phosphorylation residue on the P-domain (not shown).

After the initial submission of this manuscript, an NMR structure of the N-domain of rat α1 Na,K-ATPase was published.[20] A comparison of the two structures reveals many similarities, but also that they differ in many respects. The NMR structure is a six-stranded β-sheet, compared to the seven-stranded β-sheet of the crystallographic structure, and the structure-based sequence alignments with Ca-ATPase structure (Figure 3) differ in some regions. An interesting similarity is that the NMR structure also indicated disorder in the Glu397-Ala402 region and lack of resonances for two residues in the Phe475-Lys480 region. This shows that the lack of defined structure in these regions is not an artefact of the methods used to determine the structure or a property of the crystal. Moreover, since it appears in two different Na,K-ATPases, it is probably a general phenomenon and not a property peculiar to the species or isoform studied. In general, the helical segments are longer in the crystallographic structure than in the NMR structure. Some of the residues indicated as conserved in the NMR-based alignment of Na,K-ATPase and Ca-ATPase sequences were found to be non-homologous due to differing backbone structure in the crystallography-based alignment (Figure 3).

The NMR study[20] demonstrates that the binding of ATP to the N-domain is very weak, and far below the affinity displayed by the intact ion pump. The weak binding explains why no nucleotide could be visualised through co-crystallisation or crystal soaking with nucleotides. The NMR study demonstrated only one hydrogen bond to the ligand, which is formed by Gln482 and the adenine ring. This residue is found on the right side of the hydrophobic pocket, behind Phe475 in Figure 4(a), but is not conserved in Ca-ATPase. The lack of detectable interactions between ATP and Arg544 is also surprising; both Arg544 and its homologue Arg560 are essential for ATP binding in both

**Figure 4**. Grasp representations of the Na,K-ATPase N-domain. The Phe475-Lys480 hairpin has been modelled after Ca-ATPase[6] prior to the construction of these surfaces. The N-terminal methionine residue and the His tag were not used in the calculations but can be seen as stick representations at the bottom of the Figures. (a) Hydrophobic residues have been mapped in yellow on the surface and the positions of some of them are indicated. (b) Electrostatic potential of the surface with negative and positive charge shown in red and blue, respectively. The positions of some hydrophilic residues and Ala444 (which contributes to the charge pattern through the backbone) are indicated. Backbone and fully charged side-chain residues were used to calculate charges. (c) Residues that are identical or similar (according to Figure 3) in porcine Na,K-ATPase $\alpha_2$ N-domain and rabbit sarcoplasmic reticulum Ca-ATPase are shown in deep and light magenta, respectively.

**Table 1.** Data collection statistics for the entire resolution range and the high-resolution shell of the Na,K-ATPase N-domain crystal data set

| Resolution (Å) | 20.0–2.6 | 2.74–2.60 |
|---|---|---|
| *Data set statistics* | | |
| No. of unique reflections | 8238 | 1199 |
| Completeness (%) | 99.7(%) | 100.0 |
| $R_{sym}$ (%) | 6.8 | 30.0 |
| Multiplicity | 5.8 | 5.3 |
| $I/\sigma$ | 9.3 | 2.6 |
| *Refinement statistics* | (20–2.6 Å) | |
| *R* factor | 0.251 | |
| $R_{free}$ | 0.292 | |
| No. protein atoms | 1522 | |
| No. solvent atoms | 91 | |
| *rmsd values* | | |
| Bond length (Å) | 0.007 | |
| Bond angles (deg.) | 1.4 | |
| Dihedral (deg.) | 23 | |
| Impropers (deg.) | 0.94 | |
| $B_{ave}$ values (Å$^2$) | | |
| Protein | 45 | |
| Solvent | 48 | |

The space group was *F*23 ($a = 147.3$) with one molecule per asymmetric unit. Data statistics for the in-house data sets and phasing statistics have been published elsewhere.[22]

Na,K-ATPase and Ca-ATPase.[18,21] A number of interactions enabled the authors to place the adenine base behind the Phe475-Lys480 loop, and the ribose ring close to Ala503. This binding site is too far away from the phosphorylation residue to permit a direct transfer of the γ-phosphate group. There are several possible explanations for this; further conformational changes of the protein could be required in order to reach Asp369, or the formation of an altered, productive ATP-protein complex might require the assistance of the P-domain.

## Materials and Methods

Porcine $\alpha_2$ N-domain was purified, crystallised and analysed crystallographically as previously described.[22] In brief, phases were calculated from a mercury derivative with five heavy-atom sites with a phasing power of 1.8 and an $R_{Cullis}$ of 0.63. The figure of merit of the single isomorphous replacement (SIR) phases was improved from 0.38 to 0.89 through solvent flipping as described, and the structure was built after the resulting 3.2 Å electron density maps. The structure was refined preliminarily against in-house 3.1 Å data with the CNS program package[23] and displayed with the graphics program O.[24] For the final refinement, synchrotron data were collected at Maxlab in Lund, beam station I711 with $\lambda = 1.094$ Å using an MAR CCD detector. The oscillation angle was 0.5° and images were indexed, processed and reduced using MOSFLM,[25] and SCALA and TRUNCATE from the CCP4 program suite.[26] Data statistics from data collection and structure refinement are shown in Table 1. The Wilson *B* value was calculated from 2.6 Å to 3.2 Å data to 60 Å$^2$. $R_{free}$[27] was monitored using 5% of the data and the same selection was used for both in-house and synchrotron data. Due to the wealth of literature on porcine $\alpha_1$ Na,K-ATPase, the same residue numbering is used to describe the structure of the $\alpha_2$ isoform. Consequently, there is no residue 491 in the $\alpha_2$ protein structure. The fragment ends after Asp586 with a $His_6$ tag, where the six histidine residues have been numbered 587–592, although they cannot be regarded as homologous to any part of the natural protein. Most of the main chain is well defined; however, there are three loops where the weakness of the electron density prohibited molecular building, resulting in somewhat high *R*-values. These regions are Glu397-Ala402 and Lys428-Val436, which are close to each other, and Phe475-Lys480. In the surface representations shown in Figure 4(a)–(c), the Phe475-Lys480 loop was built manually after the homologous loop in Ca-ATPase. The distances between the $S^{\gamma}$ atoms of cysteine residues in the refined model and the heavy-atom positions in the mercury derivative are 2.8 Å (Cys421), 2.0 Å (Cys452), 2.4 Å (Cys457), 2.5 Å (Cys511) and 2.2 Å (Cys549). In the Ramachandran plot, 83.5% of the residues are found within the most favoured region and the remaining 16.5% in the additionally allowed regions. Coordinates for modelled Phe475-Lys480 loop can be requested from the author through e-mail.

### Protein data bank accession code

The crystal structure coordinates and diffraction data have been deposited with the Protein Data Bank[28] and have the accession code 1Q3I.

## Acknowledgements

The Danish research council and the Carlsberg foundation are thanked for financial support. Professor Sine Larsen is thanked for sharing synchrotron beam time. The synchrotron data were collected at the Maxlab beamstation I711 under the supervision of Dr Yngve Cerenius. Professors Peter L. Jorgensen and Per A. Pedersen are thanked for helpful and stimulating discussions.

## References

1. Skou, J. C. (1957). The influence of some cations on an adenosine triphosphatase from peripheral nerves. *Biochim. Biophys. Acta*, **23**, 394–401.
2. Kaplan, J. H. (2002). Biochemistry of Na,K-ATPase. *Annu. Rev. Biochem.* **71**, 511–535.
3. Jorgensen, P. L., Hakansson, K. O. & Karlish, S. J. (2003). Structure and mechanism of Na,K-ATPase: functional sites and their interactions. *Annu. Rev. Physiol.* **65**, 817–849.
4. Jorgensen, P. L. & Andersen, J. P. (1988). Structural basis for E1-E2 conformational transitions in Na,K-pump and Ca-pump proteins. *J. Membr. Biol.* **103**, 95–120.
5. Jorgensen, P. L. (1975). Purification and characterization of (Na +, K +)-ATPase. V. Conformational changes in the enzyme transitions between the Na-form and the K-form studied with tryptic digestion as a tool. *Biochim. Biophys. Acta*, **401**, 399–415.
6. Toyoshima, C., Nakasako, M., Nomura, H. & Ogawa, H. (2000). Crystal structure of the calcium pump of

sarcoplasmic reticulum at 2.6 Å resolution. *Nature*, **405**, 647–655.
7. Toyoshima, C. & Nomura, H. (2002). Structural changes in the calcium pump accompanying the dissociation of calcium. *Nature*, **418**, 605–611.
8. Deguchi, N., Jorgensen, P. L. & Maunsbach, A. B. (1977). Ultrastructure of the sodium pump. Comparison of thin sectioning, negative staining, and freeze-fracture of purified, membrane-bound ($Na^+$,$K^+$)-ATPase. *J. Cell Biol.* **75**, 619–634.
9. Hebert, H., Purhonen, P., Vorum, H., Thomsen, K. & Maunsbach, A. B. (2001). Three-dimensional structure of renal Na,K-ATPase from cryo-electron microscopy of two-dimensional crystals. *J. Mol. Biol.* **314**, 479–494.
10. Xu, C., Rice, W. J., He, W. & Stokes, D. L. (2002). A structural model for the catalytic cycle of $Ca^{(2+)}$-ATPase. *J. Mol. Biol.* **316**, 201–211.
11. Rice, W. J., Young, H. S., Martin, D. W., Sachs, J. R. & Stokes, D. L. (2001). Structure of $Na^+$,$K^+$-ATPase at 11-Å resolution: comparison with $Ca^{2+}$-ATPase in E1 and E2 states. *Biophys. J.* **80**, 2187–2197.
12. Hinz, H. R. & Kirley, T. L. (1990). Lysine 480 is an essential residue in the putative ATP site of lamb kidney (Na,K)-ATPase. Identification of the pyridoxal 5′-diphospho-5′-adenosine and pyridoxal phosphate reactive residue. *J. Biol. Chem.* **265**, 10260–10265.
13. Tran, C. M., Scheiner-Bobis, G., Schoner, W. & Farley, R. A. (1994). Identification of an amino acid in the ATP binding site of $Na^+/K^{(+)}$-ATPase after photochemical labeling with 8-azido-ATP. *Biochemistry*, **33**, 4140–4147.
14. Wang, K. & Farley, R. A. (1992). Lysine 480 is not an essential residue for ATP binding or hydrolysis by Na,K-ATPase. *J. Biol. Chem.* **267**, 3577–3580.
15. Ellis-Davies, G. C. & Kaplan, J. H. (1993). Modification of lysine 501 in Na,K-ATPase reveals coupling between cation occupancy and changes in the ATP binding domain. *J. Biol. Chem.* **268**, 11622–11627.
16. Farley, R. A., Heart, E., Kabalin, M., Putnam, D., Wang, K., Kasho, V. N. & Faller, L. D. (1997). Site-directed mutagenesis of the sodium pump: analysis of mutations to amino acids in the proposed nucleotide binding site by stable oxygen isotope exchange. *Biochemistry*, **36**, 941–951.
17. Maruyama, K., Clarke, D. M., Fujii, J., Inesi, G., Loo, T. W. & MacLennan, D. H. (1989). Functional consequences of alterations to amino acids located in the catalytic center (isoleucine 348 to threonine 357) and nucleotide-binding domain of the $Ca^{2+}$-ATPase of sarcoplasmic reticulum. *J. Biol. Chem.* **264**, 13038–13042.
18. Jacobsen, M. D., Pedersen, P. A. & Jorgensen, P. L. (2002). Importance of Na,K-ATPase residue alpha 1-Arg544 in the segment Arg544-Asp567 for high-affinity binding of ATP, ADP, or MgATP. *Biochemistry*, **41**, 1451–1456.
19. Kubala, M., Hofbauerova, K., Ettrich, R., Kopecky, V., Jr, Krumscheid, R., Plasek, J. *et al.* (2002). Phe(475) and Glu(446) but not Ser(445) participate in ATP-binding to the alpha-subunit of Na(+)/K(+)-ATPase. *Biochem. Biophys. Res. Commun.* **297**, 154–159.
20. Hilge, M., Siegal, G., Vuister, G. W., Guntert, P., Gloor, S. M. & Abrahams, J. P. (2003). ATP-induced conformational changes of the nucleotide-binding domain of Na,K-ATPase. *Nature Struct. Biol.* **10**, 468–474.
21. Hua, S., Ma, H., Lewis, D., Inesi, G. & Toyoshima, C. (2002). Functional role of "N" (nucleotide) and "P" (phosphorylation) domain interactions in the sarcoplasmic reticulum (SERCA) ATPase. *Biochemistry*, **41**, 2264–2272.
22. Haue, L., Pedersen, P. A., Jorgensen, P. L. & Hakansson, K. O. (2003). Cloning, expression, purification and crystallisation of the N-domain from the α2-subunit of the membrane spanning Na,K-ATPase protein. *Acta Crystallog. sect. D*, **59**, 1259–1261.
23. Brunger, A. T., Adams, P. D., Clore, G. M., DeLano, W. L., Gros, P., Grosse-Kunstleve, R. W. *et al.* (1998). Crystallography & NMR system: a new software suite for macromolecular structure determination. *Acta Crystallog. sect. D*, **54**, 905–921.
24. Jones, T. A., Zou, J.-Y., Cowan, S. W. & Kjeldgaard, M. (1991). Improved methods for building protein models in electron density maps and the location of errors in these models. *Acta Crystallog. sect. A*, **47**, 110–119.
25. Leslie, A. G. W. (1992). *Joint CCP4 and EACMB Newsletter Protein Crystallog.* **26**.
26. Collaborative Computational Project Number 4 (1994). The CCP4 suite: programs for protein crystallography. *Acta Crystallog. sect. D*, **50**, 760–763.
27. Brünger, A. T. (1992). The free *R*-value: a novel statistical quantity for assessing the accuracy of crystal structures. *Nature*, **355**, 472–474.
28. Bernstein, F. C., Koetzle, T. F., Williams, G. J., Meyer, E. E., Jr, Brice, M. D., Rodgers, J. R. *et al.* (1977). The Protein Data Bank: a computer-based archival file for macromolecular structures. *J. Mol. Biol.* **112**, 535–542.
29. Carson, M. (1991). Ribbons 2.0. *J. Appl. Crystallog.* **24**, 958–961.

***Edited by R. Huber***

*(Received 12 May 2003; received in revised form 24 July 2003; accepted 29 July 2003)*